ELSEVIER

Journal of Nuclear Materials 219 (1995) 101–109

journal of nuclear materials

Investigation of incubation time for sub-critical crack propagation in SiC–SiC composites ☆

A. El-Azab, N.M. Ghoniem

Mechanical, Aerospace and Nuclear Engineering Department, 46-147G Eng. IV, University of California, Los Angeles, Los Angeles, CA 90024, USA

Abstract

The effects of fiber thermal creep on the relaxation of crack bridging tractions in SiC–SiC ceramic matrix composites (CMCs) is considered in the present work, with the objective of studying the time-to-propagation of sub-critical matrix cracks in this material at high temperatures. Under the condition of fiber stress relaxation in the bridging zone, it is found that the crack opening and the stress intensity factor increase with time for sub-critical matrix cracks. The time elapsed before the stress intensity reaches the critical value for crack propagation is calculated as a function of the initial crack length, applied stress and temperature. Stability domains for matrix cracks are defined, which provide guidelines for conducting high-temperature crack propagation experiments.

1. Introduction

Ceramic matrix fiber composites (CMCs) such as SiC–SiC materials are under consideration for high-temperature structural applications. This class of materials shows noncatastrophic failure behavior which is characterized by fiber bridging of matrix cracks and energy dissipation by debonding and frictional fiber pull-out. These effects qualify CMCs to be classified as high toughness materials. Recent interests in using SiC–SiC composites as structural materials for high heat flux and blanket components in fusion power reactors [1] have raised some questions about the high-temperature toughness issues and high-temperature crack propagation in such materials. At elevated temperatures, creep is expected to influence the stability and propagation of matrix cracks in SiC–SiC composites. In a fusion environment, other inelastic effects such as irradiation creep and swelling are also expected to affect the composite toughness [2–4].

Experimental investigations of high-temperature crack propagation in SiC–SiC composites are underway [5]. Preliminary results have been explained in terms of conventional crack bridging models for fiber composite materials [6], which used simplified bridging relations to study the relaxation of fiber stresses in the bridging zone. In general, the results reported by Henager and Jones [6] demonstrated that SiC–SiC composites can withstand applied stress intensity factors between 20 and 25 MPa $m^{-1/2}$ without catastrophic crack propagation, at 1100°C. The material, rather, exhibited sub-critical crack growth at speeds in the range 10^{-8}–10^{-7} m s^{-1} [6]. The reported crack growth speeds were calculated, rather than directly measured, based on the assumption that the specimen compliance change is totally due to crack growth.

A theoretical model was developed to analyze the high-temperature crack propagation data in SiC–SiC composites [6]. Although the model identifies fiber creep in the bridging zone as the growth controlling mechanism, the model details and assumptions did not account for a number of factors, which include the following:

(1) Fiber–matrix interface debonding upon initial crack loading, and the time evolution of the debond

☆ Work supported by the US Department of Energy under contract number DE-FG03-91ER54115.

SSDI 0022-3115(94)00396-3

profile were not considered. Thus, the effects of the interface bonding and frictional characteristics on the behavior of matrix cracks were ignored.

(2) The crack length and the applied load were not included in the developed model.

(3) The bridging model was too simple. It considered fiber creep only in a local sense at the matrix crack face, while fiber creep must be considered, at least, over the debond/slip zone.

(4) The definition of the bridging stress as given by Henager and Jones [6] was not adequate to find the effective crack tip shielding due to fiber bridging.

The objective of the present work is to analyze the stability of matrix cracks which are bridged by creeping fibers in Nicalon–CVD SiC composites. The creep characteristics of SiC fibers and CVD SiC are reviewed in Section 2. An outline of the bridged crack model used in the present analysis is included in Section 3. A brief discussion of the micromechanical analysis used to obtain the bridging stress is included in Section 4. The time-to-crack propagation (incubation time) for a sub-critical bridged matrix crack is investigated. The main results are summarized in Section 5, followed by some concluding remarks in Section 6.

2. Creep characteristics of SiC fibers and CVD SiC

CVD SiC has been tested for creep in compression in the temperature range 1550 to 1750°C [7] and in bending in the range 1200 to 1500°C [8]. The latter creep data are considered here, and are shown in Fig. 1. The creep rate of CVD SiC in compression exhibits a power law dislocation mechanism-type creep with a stress exponent of 2.5, while the data of Gulden and

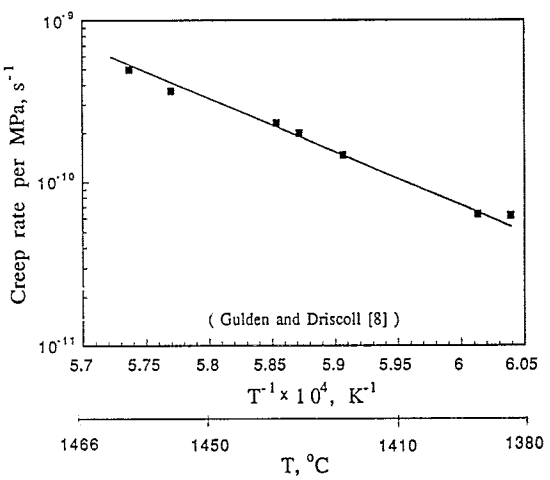

Fig. 1. Thermal creep rate of CVD SiC as function of temperature.

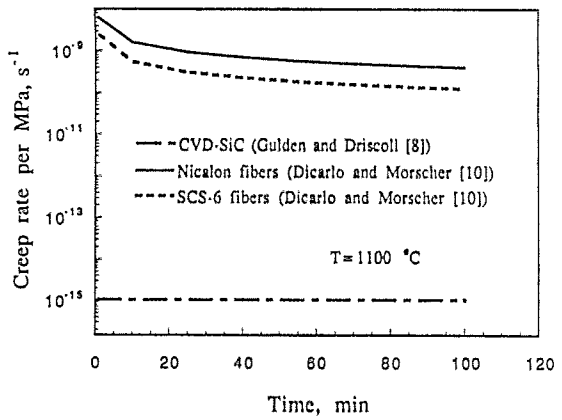

Fig. 2. Thermal creep rates of CVD SiC, Nicalon and SCS-6 fibers at 1100°C.

Driscoll [8] exhibited a diffusional creep law of the form:

$$\dot{\varepsilon}_c = \frac{13.3\sigma D\Omega_a}{kTd_g^2}, \tag{1}$$

where σ is the applied stress, D is the diffusion coefficient for the rate-controlling species, Ω_a is the atomic volume, k is the Boltzmann constant, T is the absolute temperature and d_g is the grain size. An activation energy of 640 ± 88 kJ mole^{-1} was measured [8].

Creep experiments on SCS-6 SiC fibers were carried out in the temperature range 1000–1500°C [9–11]. Creep strains were observed to increase logarithmically in time, monotonically with temperature and linearly with tensile stress. Nicalon fibers were also tested for creep [10,12]. According to Ref. [10], thermal creep strain, ε_c for these two types of fibers is given, as function of stress, time and temperature by

$$\varepsilon_c = A\sigma \exp\left(-\frac{Q}{T}\right) t^p, \tag{2}$$

where, for stress in MPa, T in K and t in s, $A = 13.112$, $Q = 25\,800$ and $p = 0.36$ for SCS-6 fibers, and $A = 8.316$, $p = 0.4$ and $Q = 24\,200$ for Nicalon fibers. The constant Q has the units of temperature. The stress exponent for Nicalon fibers is slightly different from unity [10], but considered to be unity in the present analysis to allow the use of linear viscoelasticity theory.

A comparison of the thermal creep rates of CVD SiC, SCS-6 and Nicalon fibers is shown in Figs. 2 and 3. As can be deduced from these figures, the matrix creep can be totally ignored in comparison to fiber creep. In fact, by using simple rules of mixture, it can be shown that the composites creep rates can be far slower than that of single fibers. This leads to consideration of fiber creep only in the bridging zone of a

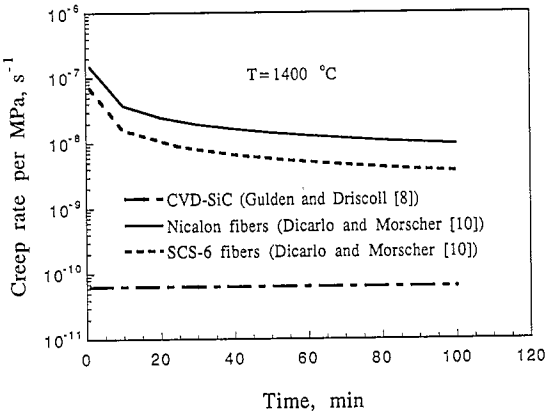

Fig. 3. Thermal creep rates of CVD SiC, Nicalon and SCS-6 fibers at 1400°C.

matrix crack, where fibers are not bonded to the matrix.

3. Bridged cracks in CMCs

Fig. 4a shows a continuum representation of a matrix crack which is bridged by fibers. In the present analysis, the singular integral equation method is used to solve the crack problem. Solutions for the crack opening displacement and the stress intensity factor follow directly from the solution of the singular integral equation. The integral equation representing the force equilibrium of a bridged crack perpendicular to the fiber direction in a unidirectional linearly elastic infinite composite, occupying the interval $-c < x < c$, is written as follows:

$$\sigma_a(x) - \sigma_B(x,t) - C_s \int_{-c}^{c} \frac{\delta'(x_0, t)}{x - x_0} dx_0 = 0, \quad |x| < c, \tag{3}$$

where $\sigma_a(x)$ is the applied stress and $\sigma_B(x,t)$ is the time-dependent bridging stress. The function $\delta'(x_0, t)$ is the gradient of the crack opening displacement. The constant C_s depends on the elastic compliance constants of the composite, s_{ij}, and is given elsewhere [13]. Singular integral equations similar to Eq. (3) are usually solved by using the Gauss–Chebyshev integration formula [14]. Due to the presence of a bridging term, which depends nonlinearly on the crack opening displacement, an iterative technique is used along with the Gauss–Chebyshev method. Once the singular integral Eq. (3) is solved for δ', the crack opening displacement $\delta(x,t)$ can then be obtained as follows:

$$\delta(x,t) = -\int_{x}^{c} \delta'(x_0, t)\, dx_0, \quad |x| < c. \tag{4}$$

The stress intensity factor, $K_I(t)$, can also be given by:

$$K_I(t) = \lim_{x \to c} \sqrt{2\pi(x-c)}\, C_s \int_{-c}^{c} \frac{\delta'(x_0, t)}{x - x_0} dx_0, \quad |x| > c. \tag{5}$$

It is to be mentioned that the bridging stress in Eq. (3) is assumed to be time-dependent due to the relaxation of fiber stress by creep at high temperature. Consequently, the crack opening displacement, $\delta(x, t)$, and the stress intensity factor, $K_I(t)$, are time-dependent.

In order to solve the singular integral Eq. (3), a definition of the bridging stress, in terms of the crack opening displacement is needed. It is known that, in ceramic matrix composites, the opening of matrix cracks under the influence of external loads is accompanied by fiber debonding and slip on the entire bridging zone. Some energy is dissipated in these two processes, which must be supplied by the external load. In addition to the direct fiber bridging, these effects must be considered. The debonding and frictional slip energy dissipation terms depend on the debond/slip profile around the matrix crack. However, since the latter

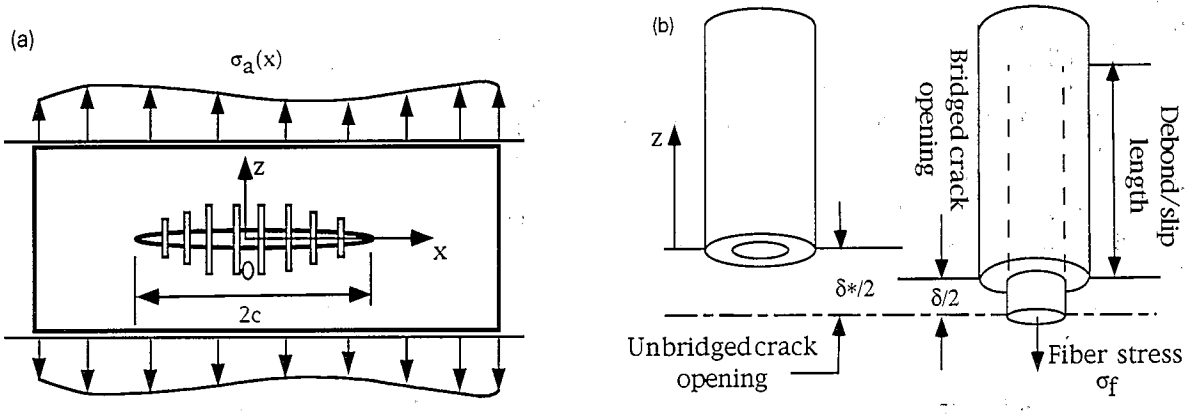

Fig. 4. (a) Continuum representation of bridged cracks. (b) Fiber–matrix micromechanics model.

depends on the crack length, it is expected that these energy terms depend on the crack length.

So far, energy dissipation by friction and debonding has been ignored in the continuum representation of bridged crack in ceramic matrix composites [15–17]. The bridging stress has been defined as the fiber stress averaged over the matrix crack by $\sigma_B = f\sigma_f$, where f is the fiber volume fraction and σ_f is the fiber stress. This definition may be valid, if fiber debonding and slip do not occur. However, since fiber debonding and slip occur during matrix crack opening, the effective bridging stress is generally different from the fiber stress averaged over the crack surface. Also, having considered only the direct effect of fiber bridging, energy dissipation by debonding and slip must be added to the critical matrix strain energy release rate (matrix fracture energy) in defining a fracture criterion. In this case, K_{IC} itself will depend on the crack size and cannot therefore be considered a fundamental material property.

In the present analysis, the critical stress intensity factor, K_{IC}, is considered to be a fundamental property and is defined by:

$$K_{IC} = \sqrt{E_c \mathscr{G}_m / \Omega}, \tag{6}$$

where $E_c = fE_f + (1-f)E_m$ is the composite modulus in the direction perpendicular to the matrix crack, E_f and E_m are respectively the fiber and matrix moduli and $\mathscr{G}_m$ is the matrix fracture energy. Ω depends on the elastic compliance constants (s_{ij}) and is given by:

$$\Omega^2 = E_c^2 s_{22}\left[2\sqrt{s_{11}s_{22}} + 2s_{12} + s_{66}\right], \tag{7}$$

A simple method to estimate the bridging stress can be illustrated as follows. Consider an *unbridged* matrix crack in which the crack opening displacement is denoted by δ^*, as shown in Fig. 4b. By applying a distribution of fiber stress $\sigma_f(x)$ on the entire crack to bring fibers from both sides of the matrix crack together, a certain interface debond/slip profile around the matrix crack develops. Also, a reduction of matrix crack opening from the unbridged state δ^* to the bridged state δ takes place. Therefore, as the fiber stress is applied, a work of $\int_{-c}^{c} f\sigma_f(x)\delta^*(x)\,dx$ is used. Ignoring friction and debonding terms, and considering the matrix crack opening from zero to a level δ against the bridging stress $\sigma_B(x)$, the work done by the bridging stress opposing crack opening is $\int_{-c}^{c}(1-f)\sigma_B(x)\delta(x)\,dx$, and the factor $(1-f)$ is included since only the matrix faces open. By equating these two terms, and considering only incremental displacements, the following expression for the local bridging stress can be obtained:

$$\sigma_B(x) = \frac{f}{1-f}\sigma_f(x)\frac{d\delta^*}{d\delta}. \tag{8}$$

This means that the bridging stress must be defined such that the work done by fiber stress through an incremental displacement $d\delta^*$ which is weighted by fiber volume fraction is equal to the work done by the corresponding bridging stress through an incremental displacement $d\delta$ and weighted by the matrix volume fraction.

El-Azab [13] has used a thermodynamical argument to derive a complete expression for the bridging stress which includes the effect of energy dissipation by debonding and frictional slip in addition to the direct fiber bridging effect. For bridged cracks in which viscoelastic effects are present, this expression is written as:

$$\sigma_B = \frac{f}{1-f}\sigma_f\frac{d\delta_e^*}{d\delta} + \frac{4f}{(1-f)R}\int_0^{\ell}\tau\frac{du_s^e}{d\delta}dz + \frac{8f}{(1-f)R}\mathscr{G}_d\frac{d\ell}{d\delta}, \tag{9}$$

in which the δ_e^* is the elastic component of fiber displacement relative to the unbridged crack surface, R is the fiber radius, τ is the interfacial friction stress along the debonded fiber–matrix interface which has a length ℓ. u_s^e is the elastic component of slip displacement along the debonded interface and $\mathscr{G}_d$ is the interface debond energy.

In order to apply the continuum theory of fracture to bridged cracks, the matrix crack must be initially closed and traction free. This is not the case, however, in CMCs due to residual stresses left from the manufacturing step. For example, for composites in which the matrix shrinks more than the fibers during cooling from the manufacturing temperature, tensile and compressive stresses exist in the matrix and fibers, respectively, in the fiber direction [13]. Once a matrix crack is formed, and prior to application of external loads, the local residual tensile stress in the matrix is relaxed at the crack face and the matrix crack tends to open. Imagine a hypothetical stress σ_i which is uniformly acting on the composite to nullify the residual matrix stress in the fiber direction. If a matrix crack is then introduced, it will be traction free and closed. In this case, the continuum mechanics of fracture can be applied, and if an external load σ_{ext} is applied to open the crack, the effective applied stress will be given by:

$$\sigma_a = \sigma_{ext} - \sigma_i. \tag{10}$$

The stress σ_i is given by:

$$\sigma_i = C_1\varepsilon_{th} = -C_1(\alpha_m - \alpha_f)\Delta T, \tag{11}$$

where ε_{th} is the residual misfit strain in the composite, α_f and α_m are the thermal expansion coefficients of fiber and matrix, respectively, and ΔT is the change from the stress-free temperature. The constant C_1 depends on the fiber volume fraction and the elastic

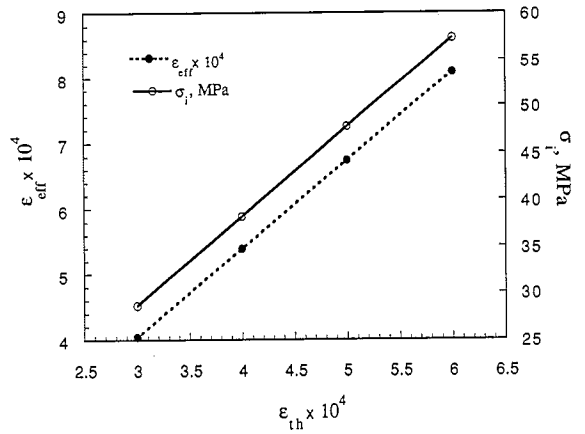

Fig. 5. Effective misfit strain, ε_{eff}, and the pre-loading stress σ_{i}, as functions of thermal misfit, ε_{th}, in Nicalon–SiC composites.

constants of fiber and matrix and is given elsewhere [13].

If the combined effect of the thermal misfit, ε_{th}, and pre-loading stress, σ_{i}, is represented by an effective misfit strain, ε_{eff}, the latter is given by:

$$\varepsilon_{\text{eff}} = C_2 \varepsilon_{\text{th}}, \tag{12}$$

where C_2 depends on the elastic constants of fiber and matrix and the fiber volume fraction. The procedure explained so far means that, the misfit strain ε_{th} will be replaced by ε_{eff} as an initial misfit, which includes the effect of the pre-loading stress σ_{i}. Also, the crack opening stress will be effectively given by $\sigma_{\text{a}} = \sigma_{\text{ext}} - \sigma_{\text{i}}$, as given by Eq. (10). Fig. 5 shows the magnitudes of ε_{eff} and σ_{i} versus the magnitude of ε_{th} for Nicalon–CVD SiC composite.

4. Micromechanics

Single fiber analysis is carried out in order to implement the definition of σ_{B}, as given by Eq. (9). This analysis includes micromechanical modeling of fiber debonding and slip processes under creep conditions. The fiber/matrix concentric cylinder model depicted in Fig. 4b is used. Details of the model are found elsewhere [13]. A summary of the basic features of the micromechanical model are outlined below.

Over the debonded length $0 < z < \ell$, where z is along the fiber direction, axial slip between fiber and matrix is allowed which is resisted by a Coulomb-type friction. In this interval, the model uses an axial equilibrium condition of the form:

$$\frac{\mathrm{d}\sigma_{\text{f}}^{z}(z)}{\mathrm{d}z} = \frac{2\mu q(z)}{R} = -\left(\frac{1-f}{f}\right)\frac{\mathrm{d}\sigma_{\text{m}}^{z}(z)}{\mathrm{d}z}, \tag{13}$$

where $\sigma_{\text{f}}^{z}(z)$ and $\sigma_{\text{m}}^{z}(z)$ are the axial fiber and matrix stresses, respectively, $q(z)$ is the interface pressure and μ is the interface friction coefficient. For $z > \ell$, where no axial slip takes place, an equilibrium condition of the form:

$$f\sigma_{\text{f}}^{z}(z) + (1-f)\sigma_{\text{m}}^{z}(z) = f\sigma_{\text{f}} \tag{14}$$

is used, where σ_{f} is the fiber stress at the matrix crack face. The stress–strain relationships for the matrix are conventional thermoelastic. The fiber stress–strain relationships, however, have the form:

$$\varepsilon_{ij} = \alpha_{\text{f}}\Delta T + \varepsilon_{ij}^{\text{e}} + \varepsilon_{ij}^{\text{c}}, \tag{15}$$

where $\alpha_{\text{f}}\Delta T$ is the fiber thermal strain, $\varepsilon_{ij}^{\text{e}}$ is the elastic strain component and $\varepsilon_{ij}^{\text{c}}$ is the creep strain component. The latter depends on the full history of fiber stresses. Due to fiber creep, all stress and strain components in fiber and matrix are time-dependent.

The crack opening displacement at a particular location along the matrix crack is defined by the net fiber pull-out from the matrix, as given below:

$$\delta = 2\int_0^{\ell}[\varepsilon_{\text{f}} - \varepsilon_{\text{m}}]\,\mathrm{d}z, \tag{16}$$

where ε_{f} and ε_{m} are the axial fiber and matrix strains. The elastic fiber displacement component at matrix crack face, δ_{e}^{*}, and the elastic slip displacement, u_{s}^{e}, which appear in Eq. (9) are defined by:

$$\delta_{\text{e}}^{*} = 2\int_0^{\ell}\varepsilon_{\text{f}}^{\text{e}}\,\mathrm{d}z,$$

$$u_{\text{s}}^{\text{e}}(z) = \int_z^{\ell}[\varepsilon_{\text{f}}^{\text{e}} - \varepsilon_{\text{m}}]\,\mathrm{d}z, \tag{17}$$

where $\varepsilon_{\text{f}}^{\text{e}}$ is the elastic component of the axial fiber strain. The fiber debonded length is found by applying energy balance principles to the debond crack, which brings in the effect of interface debonding energy, $\mathscr{G}_{\text{d}}$.

The model solution eventually yields the fiber stress, σ_{f}, the elastic fiber displacement, δ_{e}^{*}, the elastic slip displacement over the debond length, u_{s}^{e}, the interfacial friction stress, $\tau = -\mu q$, and the debond length ℓ as functions of the time-dependent crack opening displacement, δ. The relationships between these variables and the crack opening displacement δ are then used to find the bridging stress using Eq. (9).

5. Results and discussion

The model outlined in the previous sections is applied to sub-critical matrix cracks in one-dimensional Nicalon–CVD SiC composites. The fiber and matrix properties used in the present analysis are: $E_{\text{f}} = 180$ GPa, $E_{\text{m}} = 380$ GPa, $\nu_{\text{f}} = 0.2$ and $\nu_{\text{m}} = 0.18$. The Poisson's ratio of fibers during creep is $\nu_{\text{fc}} = 0.45$. The

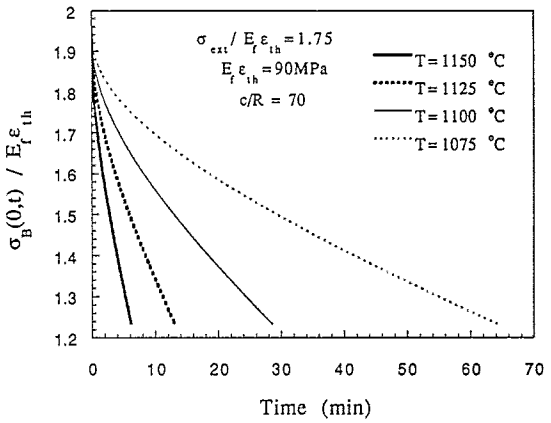

Fig. 6. Bridging stress relaxation as function of temperature.

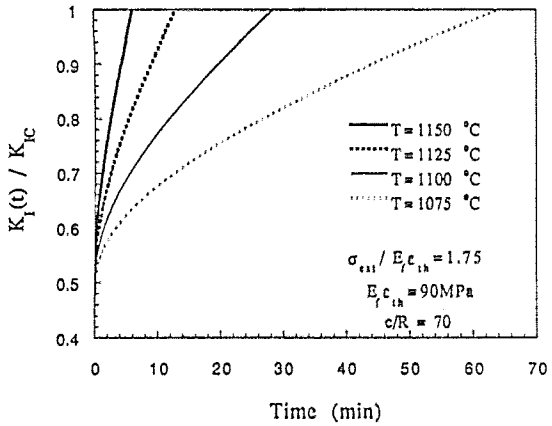

Fig. 8. Evolution of the stress intensity factor at different temperatures.

corresponding compliance constants are found to be: $s_{11} = 3.71 \times 10^{-6}$ MPa^{-1}, $s_{22} = 3.44 \times 10^{-6}$ MPa^{-1}, $s_{12} = -6.48 \times 10^{-7}$ MPa^{-1} and $s_{66} = 8.845 \times 10^{-6}$ MPa^{-1}. A fiber volume fraction of 0.4 is considered. The fiber radius is 7 μm. The interface debonding energy of $\mathcal{G}_d$ is assumed to be 5% of the matrix fracture energy $\mathcal{G}_m$. The latter is typically 50 J m^{-2}. The interface friction coefficient μ is assumed to be 0.1. These properties are adopted from El-Azab [13].

Fiber creep in the bridging zone leads to a relaxation of the bridging traction that opposes crack opening. Fig. 6 shows the time-dependent relaxation of bridging stress at the center of a bridged crack at different temperatures before the tip stress intensity reaches its critical value, K_{IC}. It is shown that, the bridging relaxation rate is faster at higher temperatures. Due to fiber bridging relaxation, the crack opening displacement and the stress intensity factor are expected to increase with time. Fig. 7 shows the time evolution of the crack opening displacement over the entire matrix crack. Initially, the crack opening profile

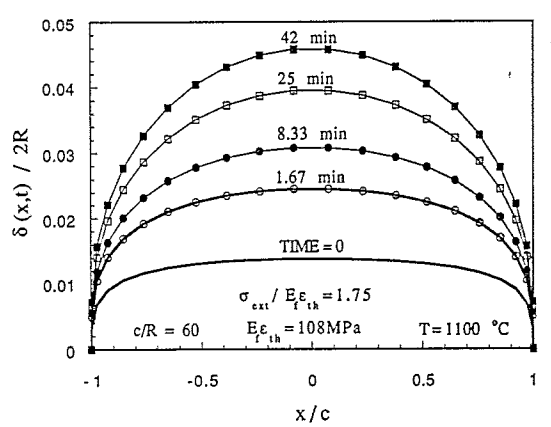

Fig. 7. Evolution of crack opening displacement under fiber creep condition.

is fairly flat in the middle section of the crack. This profile, however, approaches the unbridged crack opening as the bridging traction continues to relax by fiber creep. The important aspect to note here is that the increase of the crack opening displacement with time implies that the compliance of the cracked material is increasing although the crack itself does not propagate. This compliance increase may continue for longer times before the crack starts to propagate, depending on the initial crack length, applied stress and temperature. In Henager's experiment [6], however, the increase in compliance was interpreted in terms of crack propagation rather than fiber creep in the bridging zone.

The corresponding behavior of the crack tip stress intensity factor is shown in Fig. 8 for different temperatures. The rate of increase of the crack tip stress intensity is faster at higher temperatures since fiber creep rates are faster. Consequently, the incubation time, which is the time required for $K(t)$ to reach K_{IC}, becomes shorter at higher creep temperatures. The critical tip stress intensity factor K_{IC} is calculated to be 3.77 MPa m$^{1/2}$ based on matrix fracture energy of 50 J m^{-2} and the composite properties given previously. Although this value is slightly lower than the toughness of the monolithic SiC, the applied stresses required to raise the net crack tip stress intensity to K_{IC} may be an order of magnitude higher in the case of composites due to fiber bridging. However, under fiber creep the crack tip shielding due to fiber bridging can be gradually lost, which sets restrictions on the high temperature range in which SiC–SiC composites may be used.

The mechanisms of bridging relaxation by fiber creep can be explained by investigating the individual terms in Eq. (9). The second term (friction term) is a few times higher than the first terms, while the third term is a few orders of magnitude smaller. Creep relaxes the fiber stress, σ_f, leading to partial reduction

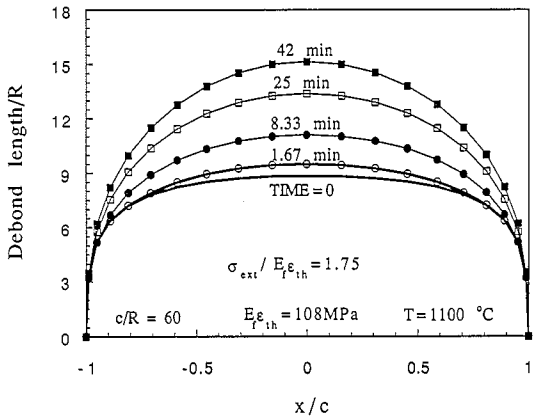

Fig. 9. Debond front evolution around matrix crack.

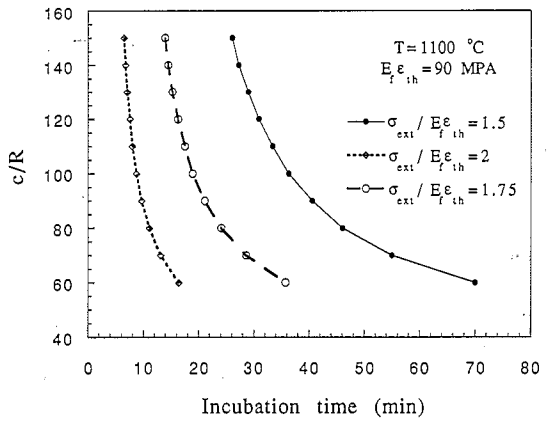

Fig. 11. Incubation time for sub-critical crack propagation as function of matrix crack length and external load.

of the bridging traction (first term). Creep also relaxes the interfacial pressure between fiber and matrix. This interface pressure controls the frictional energy dissipation associated with fiber slip (second term). While the interface pressure relaxes by creep, it actually recovers if the axial fiber stress, σ_f, relaxes due to Poisson's effect. Therefore, the relaxation of σ_f may not have a great influence on the relaxation of the bridging stress.

The debond crack tips at the fiber–matrix interface are shielded by interfacial friction. Relaxation of the interface pressure and, in turn, the interfacial friction stress allows the debond crack to grow. This debond growth depends on the interface debonding energy as well as the friction stress distribution over the debond length. Since the second term in Eq. (9) increases as the debond length ℓ increases, it may be beneficial to allow growth of debond cracks by lower values of the interface debonding energy and further controlling the interface friction characteristics. An example of the debond growth over the entire matrix crack is shown in Fig. 9.

The time-to-crack propagation (incubation time) has been shown to depend on the temperature (Fig. 8). In Fig. 10, the incubation time is plotted as function of the matrix crack length and temperature. It is observed that, depending on the matrix crack length and temperature, a wide range of incubation times can be obtained. Here we report incubation times between 5 min and 1.5 h, for crack length in the range 120–300 fiber radii, and temperature in the range 1075–1150°C. Smaller cracks at lower temperatures may exhibit incubation times of several hours or days, depending on the applied loads. The effect of the applied stress is also shown in Fig. 11. It is shown that for the same crack length, the incubation time is longer at lower applied stress.

The effect of the initial misfit strain ε_{th} on the incubation time for subcritical cracks is shown in Fig. 12. Generally, incubation times become longer for

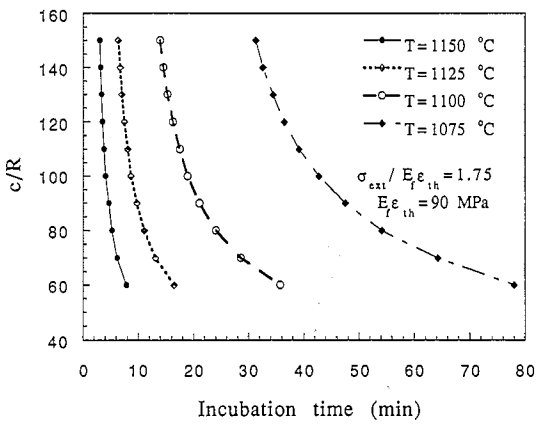

Fig. 10. Incubation time for sub-critical crack propagation as function of matrix crack length and temperature.

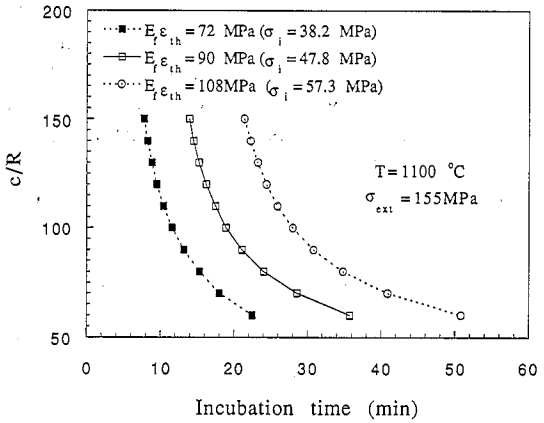

Fig. 12. Incubation time for sub-critical crack propagation as function of matrix crack length and thermal misfit strain.

higher values of ε_{th}. Based on this figure, it can be argued that a higher level of misfit strain is needed to maintain a higher bridging stress for longer times. This brings in some interesting questions about the expected behavior of SiC–SiC composites in a fusion environment, where irradiation creep is expected to occur once the material is subjected to combined mechanical and irradiation loading, even at temperatures below thermal creep threshold. Swelling rates of the fiber and matrix are expected to control the instantaneous misfit level. Consequently, the relative irradiation creep and swelling rates of the fiber and matrix must be beneficially adjusted to maintain certain levels of misfit between fiber and matrix.

In Figs. 10 through 12, the incubation times for shorter cracks are longer. There is a minimum crack length, which is determined by the effective applied stress alone, below which incubation times must be infinitely long. This limiting value is the length of an unbridged crack which satisfies the condition $K_I = K_{IC}$ at the given applied stress. This means that a horizontal asymptotic line exists for each curve on Figs. 10 through 12. These asymptotes must be the same for the same effective applied stress, σ_a, irrespective of the creep temperature. In the large crack length limit, incubation time curves tend to have asymptotic behavior too. Each curve tends to have a vertical asymptote, which means that there exists a minimum incubation time, which depends on the crack length, applied stress, and temperature, below which large cracks are sub-critical.

The plots shown in Figs. 10 through 12 are useful in two circumstances; studying crack behavior in ceramic matrix composites operating at high temperatures and designing experiments to study crack propagation in such class of materials. In the first case, designers may be interested in allowing for cracks to exist in structural components. If the lifetime of the component is specified or limited by some factor other than crack growth, then a defect tolerant design can be conducted with the help of incubation charts similar to those given in the present study, by choosing incubation times which are longer than the specified lifetime of the component. Consequently, an upper defect size limit can be tolerated. In designing crack growth experiments, the incubation charts may help choose the right combination of crack length, applied stress and temperature to run the experiment in a specific time frame.

The present analysis can be advanced to study the time-dependent deformation behavior of structural ceramic matrix composites which contain large numbers of matrix microcracks. This can be achieved by using some averaging methodology to predict the global time-dependent load-deformation of the composite using crack solution outlined here as a unit cell solution.

6. Conclusions

A study of the time-dependent behavior of sub-critical bridged crack in SiC–SiC composites at high temperatures is presented. A new concept of bridging stress is used, which considers the effects of energy dissipation in fiber debonding and frictional slip, in addition to the direct fiber bridging, on the matrix crack opening. A fracture criterion which is based on the matrix fracture energy alone, is used. The effects of the initial residual misfit strains on matrix cracking, and the subsequent crack opening evolution are considered.

It is found that the incubation time for sub-critical bridged cracks is controlled by fiber creep in the bridging zone. Maintaining specific levels of misfit strains may actually delay the relaxation of bridging tractions and, in turn, increase the incubation time of a crack for a given applied stress and creep temperature. For fusion applications, the relative swelling and irradiation creep rates of fibers and matrix will ultimately control the misfit level between fiber and matrix, and particular optimization techniques must be explored to maintain the viability of fiber bridging mechanism of toughening under fusion conditions.

For sub-critical cracks at high temperatures, the incubation time becomes shorter at higher values of applied stress and creep temperature and lower initial misfit strains. The domains of stability of high-temperature bridged cracks can be explored by systematically producing incubation charts of the type shown in Figs. 10 through 12, therefore, a SiC–SiC composite structural element can be designed for reasonably long incubation times for tolerable sizes of matrix cracks, prior to propagation.

Acknowledgement

The authors would like to acknowledge the reviewer's effort in providing valuable comments on the original manuscript.

References

[1] F. Najmabadi, R.W. Conn and the ARIES Team, The ARIES II and ARIES IV Second Stability Tokamak Reactor Study — Final Report, UCLA-PPG 1461(1994).
[2] A. El-Azab and N.M. Ghoniem, Viscoelastic Analysis of Residual Mismatch Stresses in Ceramic–Matrix Composites Under High-Temperature Neutron Irradiation, submitted to Mech. of Mater. (1993).
[3] A. El-Azab and N.M. Ghoniem, Phenomenological Inelastic Constitutive Equations for CVD SiC and SiC Fibers Under Irradiation, Fusion Technol. (1994), in press.

[4] A. El-Azab and N.M. Ghoniem, J. Nucl. Mater. 212–215 (1994) 845.
[5] R.H. Jones, C.H. Henager and G.W. Hollenberg, J. Nucl. Mater. 191–194 (1992) 75.
[6] C.H. Henager and R.H. Jones, Mater. Sci. Eng. A166 (1993) 211.
[7] C.H. Carter, Jr. and R.F. Davis, J. Am. Ceram. Soc. 67 (11) (1984) 732.
[8] T.D. Gulden and C.F. Driscoll, Creep of Chemically Vapor-Deposited β-SiC with an Analysis of Creep in Bending, Gulf General Atomic Report, GA-10366, February 16, 1971.
[9] J.A. Dicarlo, J. Mater. Sci. 21 (1986) 217.
[10] J.A. Dicarlo and G.N. Morscher, Creep and Stress Relaxation Modeling of Polycrystalline Ceramic Fibers, in Failure Mechanisms in High Temperature Composite Materials, eds. G.K. Haritos, G. Newaz and S. Mall, ASME AD-vol. 22, AMD-vol. 122 (1991) p. 15.
[11] G.N. Morscher and J.A. Dicarlo, J. Am. Ceram. Soc. 75 (1) (1992) 136.
[12] G. Simon and A.R. Bunsell, J. Mater. Sci. 19 (1984) 3658.
[13] A.A. El-Azab, Time-Dependent High-Temperature Fracture of Ceramic Matrix Composites, Ph.D. Dissertation, University of California, Los Angeles (1994).
[14] F. Erdogan, G.D. Gupta and T.S. Cook, Numerical Solution of Singular Integral Equations, in: Fracture Mechanics 1: Methods of Analysis and Solutions of Crack Problems, ed. G.C. Sih (Noordhoff, Leiden, 1973) p. 369.
[15] D.B. Marshall, B.N. Cox and A.G. Evans, Acta Metall. 33 (11) (1985) 2013.
[16] D.B. Marshall and B.N. Cox, Acta Metall. 35 (11) (1987) 2607.
[17] B.N. Cox and D.B. Marshall, Acta Metall. 39 (4) (1991) 579.